

# V-RoAst: Visual Road Assessment Can VLM be a Road Safety Assessor Using the iRAP Standard?

Natchapon Jongwiriyanurak<sup>1\*</sup>, Zichao Zeng<sup>1</sup>, June Moh Goo<sup>1</sup>, James Haworth<sup>1</sup>, Xinglei Wang<sup>1</sup>, Kerkritt Sriroongvikrai<sup>2</sup>, Nicola Christie<sup>1</sup>, Ilya Ilyankou<sup>1</sup>, Meihui Wang<sup>1</sup>, Huanfa Chen<sup>3</sup>

**1** Department of Civil, Environmental and Geomatic Engineering, University College London, London, UK

**2** Department of Civil Engineering, Chulalongkorn University, Bangkok, Thailand

**3** The Bartlett Centre for Advanced Spatial Analysis, University College London, London, UK

\* natchapon.jongwiriyanurak.20@ucl.ac.uk

## Abstract

Road traffic crashes result in millions of deaths annually and significant economic burdens, particularly on Low- and Middle-Income Countries (LMICs). Road safety assessments traditionally rely on human-labelled data, which is labour-intensive and time-consuming. While Convolutional Neural Networks (CNNs) have advanced automated road safety assessments, they typically demand large labelled datasets and often require fine-tuning for each new geographic context. This study explores whether Vision Language Models (VLMs) with zero-shot capability can overcome these limitations to serve as effective road safety assessors using the International Road Assessment Programme (iRAP) standard. Our approach, *V-RoAst* (**V**isual question answering for **R**oad **A**ssessment), leverages advanced VLMs, such as Gemini-1.5-flash and GPT-4o-mini, to analyse road safety attributes without requiring any labelled training data. By optimising prompt engineering and utilising crowdsourced imagery from Mapillary, *V-RoAst* provides a scalable, cost-effective, and automated solution for global road safety assessments. Preliminary results show that while VLMs achieve lower performance than CNN-based models, they are capable of Visual Question Answering (VQA) and show potential in predicting star ratings from crowdsourced imagery. However, their performance is poor when key visual features are absent in the imagery, emphasising the need for human labelling to address these gaps. Advancements in VLMs, alongside in-context learning such as chain-of-thought and few-shot learning, and parameter-efficient fine-tuning, present opportunities for improvement, making VLMs promising tools for road assessment tasks. Designed for resource-constrained stakeholders, this framework holds the potential to save lives and reduce economic burdens worldwide. Code and dataset are available at: <https://github.com/PongNJ/V-RoAst>.

# 1 Introduction

Road traffic crashes were estimated to cause 1.19 million deaths worldwide in 2021, with an economic impact of approximately 10-12% of the global Gross Domestic Product (GDP) [1, 2]. According to WHO [1], in low- and middle-income countries (LMICs), road crashes rank as the leading cause of death, with fatality rates significantly higher than those of high-income countries (HICs). A significant portion of these fatalities involves motorcyclists, who are among the most vulnerable road users in LMICs. Consequently, the United Nations (UN) has aimed to ensure that all new roads are built to achieve a rating of at least 3 stars according to the International Road Assessment Programme (iRAP) standard, which rates roads on a scale from 1 to 5, with 5 indicating a safe road and 1 indicating an unsafe road [1]. Furthermore, another objective is to improve 75% of existing roads to more than 3 stars by 2030.

The workflow of iRAP involves road surveys, coding attributes, developing the model, and analysing the results. From iRAP survey manual<sup>1</sup>, the process requires vehicles and sensors to capture accurate georeferenced images for coding. Once georeferenced images are obtained, trained coders must examine and classify the images according to the codebook manual<sup>2,3</sup>, which requires training and experience. Currently, only highways have been rated due to the prohibitive cost of the survey. Importantly, it is almost impossible for LMICs to assess all roads following this standard. This leaves the vast majority of the road network unrated, making it difficult to reveal the infrastructure risk factors contributing to road deaths.

Although Accelerated and Intelligent RAP (AiRAP<sup>4</sup>) has initiated several programmes to help provide tools and attributes to local authorities, these programmes do not cover all cities and countries and come with associated costs. To save costs, automated road feature detection directly from captured images is a well-known approach that primarily employs models based on Convolutional Neural Networks (CNN). Although they are inexpensive compared to manual labelling, these models require labelled data for training, which is time-consuming and limits region-scalability since road attributes can visually vary in different cities and countries [3, 4, 5, 6, 7]. Additionally, some studies explore alternative data sources, such as Light Detection and Ranging (LiDAR) [8], satellite imagery [9, 10], Unmanned Aerial Vehicles (UAV) [11], and Global Positioning System (GPS) traces [12].

Recently, many researchers have explored the performance of Visual Language Models (VLMs) on various computer vision tasks. Since VLMs have been trained on large datasets of images and texts, they can perform tasks without additional model training. Recently, techniques such as prompt engineering, Retrieval-Augmented Generation (RAG) [13], and fine-tuning [14] have been explored to enhance the potential of VLMs, as building these models requires significant computational resources and datasets. Furthermore, VLMs have shown their potential to handle

---

<sup>1</sup>[https://resources.irap.org/Specifications/iRAP\\_Survey\\_Manual.pdf](https://resources.irap.org/Specifications/iRAP_Survey_Manual.pdf)

<sup>2</sup>[https://resources.irap.org/Specifications/iRAP\\_Coding\\_Manual\\_Drive\\_on\\_Left.pdf](https://resources.irap.org/Specifications/iRAP_Coding_Manual_Drive_on_Left.pdf)

<sup>3</sup>[https://resources.irap.org/Specifications/iRAP\\_Coding\\_Manual\\_Drive\\_on\\_Right.pdf](https://resources.irap.org/Specifications/iRAP_Coding_Manual_Drive_on_Right.pdf)

<sup>4</sup><https://irap.org/project/ai-rap>

complex tasks using zero-shot learning, such as building age classification [15], building detection [16], motorcycle risk assessment [17], land use classification [18], and building defects detection [19]. However, VLMs' zero-shot prediction and generalisation ability on the road feature detection task is still unknown. Therefore, this work focuses on the potential of using VLMs to assist in road assessment.

This study develops prompts for VLMs to examine iRAP attributes by mimicking a coder observing an image and categorising the attributes, as described in codebook manual. Additionally, we evaluate the feasibility of leveraging the zero-shot capabilities of VLMs for this task, assuming the models are sufficiently advanced for practical application. In summary, we state the main contributions of our work as follows:

- **Novel Task Definition:** We propose a new image classification task for VLMs with a real-world dataset from **ThaiRAP**
- **Prompt Optimisation:** We optimise the prompts and evaluate the potential of using VLMs to code road attributes using Gemini-1.5-Flash and GPT-4o-mini compared to traditional computer vision models
- **Zero-Shot Classification:** We demonstrate that VLMs can classify iRAP attributes with zero-shot capabilities, although with lower performance than VGGNet and ResNet. However, there is room to improve classification accuracy by applying in-context learning and fine-tuning, which might require a larger dataset.
- **Scalable Assessment Framework:** We present a scalable approach using crowdsourced imagery, Mapillary<sup>5</sup>, to estimate star ratings.

## 2 Literature review

### 2.1 Computer Vision for Road Attribute Detection and Classification

Using engineers to survey, inspect, and assess roads on-site is time-consuming and costly. Therefore, various studies have explored the use of computer vision models to assist in specific tasks, such as crack detection [20], pothole detection [21], and pavement distress detection [22].

Similarly, examining road attributes following the iRAP standards has been dramatically advanced using images and videos. The availability of the AusRAP dataset with labelled street objects has enabled the development of models to detect street attributes. However, due to the limitations of visual scenes from videos and the feasibility of labelling objects (e.g., lane lines, rumble strips, poles, trees, barriers, and speed signs), only 13 attributes were able to be classified [4, 5, 6].

In terms of model architectures, Fully Convolutional Networks (FCNs) effectively segmented objects and defined attributes from images [7]. Song et al.[23] automated the process using star ratings from ground-level panoramic images. They developed a VGG-based model that incorporated a task-dependent spatial attention layer, which was trained using a supervised multi-task learning approach. However, the task primarily focused on predicting star rating scores rather than coding road attributes. Some studies have proposed multi-task convolutional models that utilise

<sup>5</sup><https://www.mapillary.com/developer/api-documentation>

monocular videos to predict 33 attributes [3, 24]. Nevertheless, all these studies required large amounts of training data with dense pixel-level annotation, indicating considerable annotation effort and substantial computational resources.

In addition, due to dataset imbalance, these works struggle with certain road features, such as pedestrian fencing and facilities for motorcycles and bicycles. Consequently, some attributes experience the problem of Out-Of-Distribution (OOD), i.e., some attributes have classes with only a small amount of data or even missing data [25]. This makes multi-attribute classification more challenging. Hence, these models require significant additional training data, even when using transfer learning or semi-supervised learning approaches.

In conclusion, previous works benefit from the availability of labelled datasets and can detect, segment, and classify attributes required for automated road assessments. Traditional computer vision models show limitations on datasets with OODs due to overfitting to the majority classes of the distribution[25].

## 2.2 Visual Language Models

In recent years, Large Visual Language Models (LVLMs) have become significantly important in the computer vision domain. VLMs can process image and text inputs and produce text outputs that can be used in many tasks, such as image captioning, image-text matching, visual reasoning, and visual question answering (VQA). LVLMs have been extensively developed by leading researchers using large amounts of text and image datasets with different architectures. Examples include GPT 4o [26], Gemini 1.5 [27], CogVLM2 [28], LLaVA [29], LLaMA [30] and QwenVL [31]. These models have been evaluated for their potential to outperform several traditional deep learning state-of-the-art benchmarks, including 3D object generation [32], and image segmentation [33]. However, these models come with different licences, costs, and limitations.

VLMs have also been trained, fine-tuned, and validated to understand street scenes, primarily focusing on the autonomous driving domain [34, 35, 36, 37, 38]. These models mainly focus on controlling, object detection, and depth estimation rather than captioning street scenes. Besides, Wen et al. [39] explored GPT-4vision and demonstrated its great potential for understanding street scenes by captioning images as one of the tasks for autonomous driving. However, challenges remain in traffic light recognition, vision grounding, and spatial reasoning tasks. Luo et al. [40], on the other hand, explored foundation models for understanding road scenes with the potential usage of existing road scene datasets. Moreover, for finer-grained image understanding, Zeng et al.[15] used GPT-4 to extract building features and classify building attributes from the street imagery without training data. These works demonstrated the potential of VLMs for zero-shot understanding of road images, which can be an alternative for automated road feature detection with OOD problems. Inspired by them, in this study, we explore the attribute coding capabilities of VLMs.

### 2.3 VQA

Visual Question Answering (VQA) was initially introduced as a new task in the computer vision and natural language processing domains [41]. The task involves answering open-ended questions based on images. Several datasets are commonly used to evaluate models, including GQA [42], OK-VQA [43], A-OKVQA [43], and MMMU [44].

In addition, VQA datasets focusing on autonomous vehicles, such as KITTI [45] and NuScenes-QA [46], have been used to advance the field. Jain et al. [47] found that GPT-4 performs well in robust driving scenarios.

This work uses a real-world dataset to define a new image classification dataset for VLMs as a downstream vision application. It does not consider training a new VLM but instead explores the potential of existing LLMs to perform the task as road assessment coders. Although using non-open-source models incurs some costs, this study aims to demonstrate that coding road assessments can benefit from existing LLMs. It also allows for applying prompt engineering, RAG, and fine-tuning.

## 3 Dataset

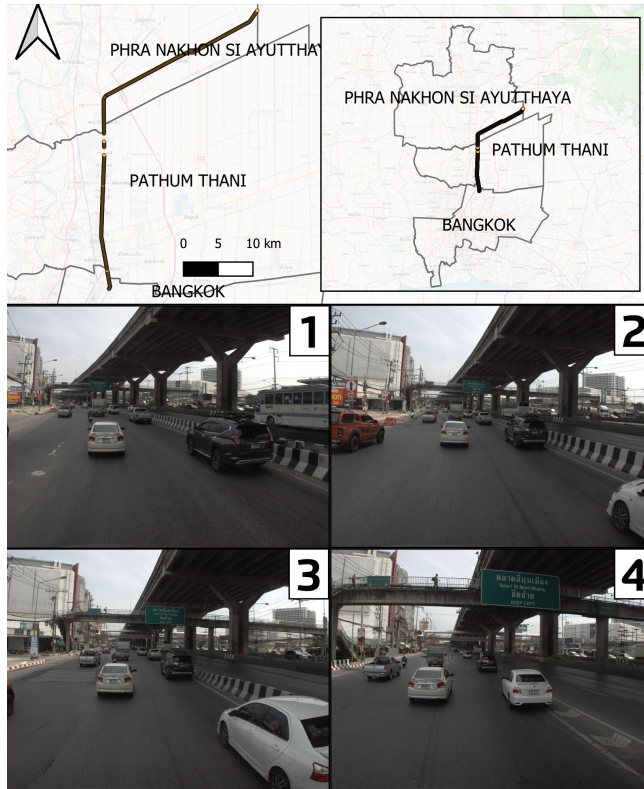


**Fig 1.** Locations of the ThaiRAP dataset and an example of images in a road segment. The numbers on the images indicate their order within the section.

### 3.1 Dataset Collection

The dataset used in this work is sourced from the ThaiRAP and was selected due to the availability of road assessment datasets following the iRAP standard. The experiment includes 2,037 images (1600x1200 pixels) captured across 3 provinces, including Bangkok, Pathum Thani, and Phranakorn Sri Ayutthaya, as illustrated in Figure 1. These images represent 519 road segments, with 1-4 images used to code each 100-metre segment. While iRAP datasets are typically not publicly available, this work will provide access to the ThaiRAP dataset, including both the images and their associated attributes defined by trained coders (professionals responsible for coding road attributes for iRAP assessments) to support further research and development in road safety assessment.

### 3.2 Dataset Annotation

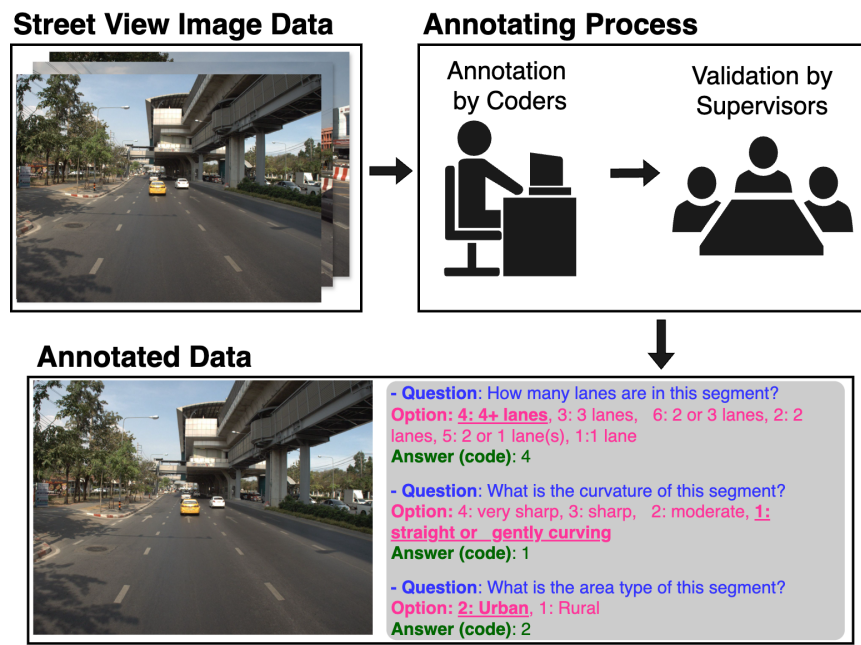


Fig 2. V-RoAst Dataset Annotation Process

The dataset comprises street-level imagery annotated by qualified road safety engineers (coders) according to iRAP standards, as shown in figure 2. Each image segment goes through a systematic review, during which coders identify key road attributes, such as the number of lanes, roadway curvature, and area type. For instance, coders record whether the segment contains multiple lanes (e.g., four, three, two), assess the degree of curvature (e.g., very sharp, sharp, moderate, gently curving), and specify the surrounding environment (e.g., urban or rural).

### 3.3 Dataset Statistics

Each segment has 52 attributes classified by the coding manual. However, the attributes have a different number of classes (codes) in parentheses, and the number of classes of each attribute used in this experiment is

shown at the top of each bar in Figure 3. This dataset shows the imbalance of classes of attributes, in which there are 11 attributes with only one class. Since only one attribute class is available, we cannot build supervised models. Some classes have fewer than 10 samples. Additionally, some attributes do not appear with all possible classes. For example, the “Bicycle Observed Flow” attribute might only have 6 valid classes in the dataset, while “Centreline rumble strips” might only have 2.

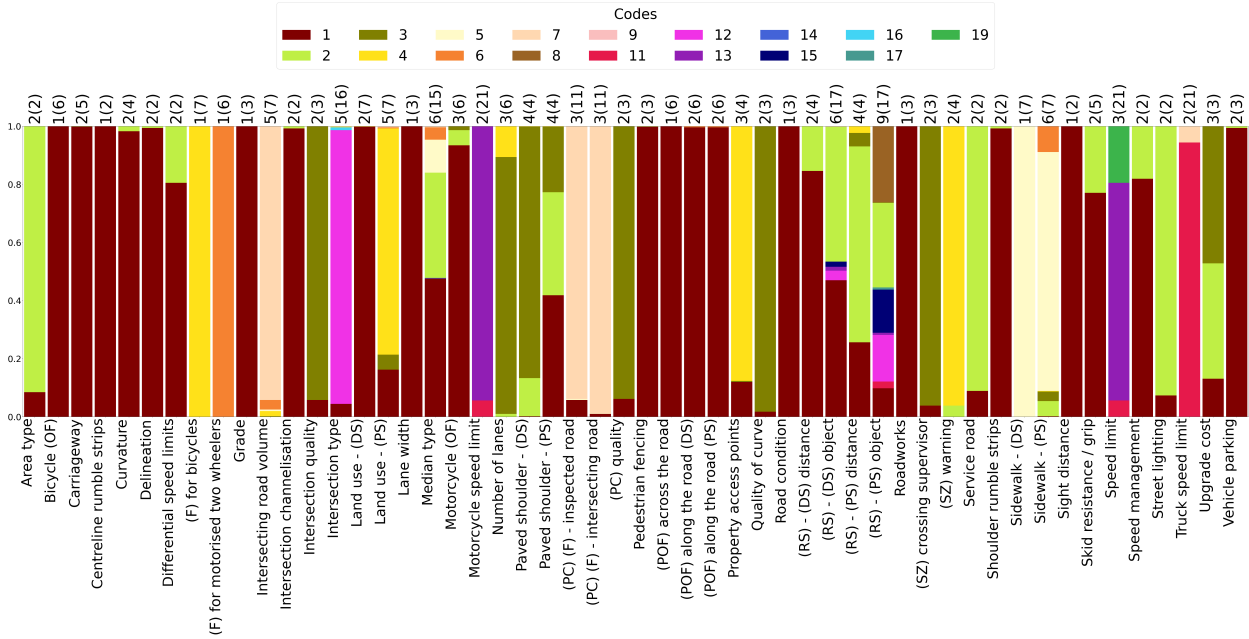


**Fig 3.** Code distribution: the numbers at the top indicate the unique codes (representing all possible codes). The following abbreviations are used: (OF) = Observed Flow, (F) = Facilities, (DS) = Driver-Side, (PS) = Passenger-Side, (PC) = Pedestrian Crossing, (POF) = Pedestrian Observed Flow, (RS) = Roadside Severity, (SZ) = School Zone.

## 4 Methodology and Experiments

### 4.1 Data preprocessing

To evaluate and compare our models against the baseline models - traditional computer vision methods, we divide the dataset ( $n=2037$ ) into a training set (1274 original samples + 464 augmented samples), a testing set (492 samples), a validation set (243 samples), and an unseen set (28 samples). The dataset is split by ensuring a balanced distribution across subsets, maintaining sample sizes for each class within the attribute. The data split follows these rules: 1. Attributes with only one class are ignored; 2. Classes with more than 4 but fewer than 12 samples are augmented; 3. Classes with 4 or fewer samples are augmented if their attributes have only 2 classes; 4. Samples from classes with 4 or fewer samples are moved to the unseen set if their attributes have more than 2 classes.

For rules 2 and 3, we generated noise-added data and added them to the training dataset to alleviate the class imbalance problem in our dataset. Specifically, we add 5 different types of noise: Gaussian noise, salt and

pepper noise, speckle noise, periodic noise, and quantisation noise for each selected image. For rule 4, the unseen set is used to test the zero-shot prediction capacities in unseen classes. The baseline models have been trained on the training set and monitored by the validation set. The performance of our models and the baseline models are evaluated in the testing and unseen sets.

## 4.2 Baseline

**VGGNet** [48] is a deep neural network model known for its simple architecture that stacks multiple convolutional layers with small 3x3 filters, achieving high performance in image classification tasks and becoming a widely used baseline in computer vision.

**ResNet** [49] is also a deep convolutional neural network that utilises residual blocks and skip connections to enhance feature learning at various abstraction levels, making it highly effective for image classification and transfer learning tasks.

Our study uses VGGNet and ResNet as baseline models to compare with our proposed approach. These models were selected because they have been widely used in previous work on road safety assessment and multi-task classification [3, 23]. Since they are designed for single-task classification, we adapt the architectures for a multi-attribute coding problem, where a single encoder is shared across all tasks, and separate decoders are allocated for each individual task.

It is important to note that this study focuses on evaluating the potential of VLMs with zero-shot learning for road safety assessment. Therefore, we do not include all existing computer vision approaches, such as Vision Transformers (ViT)[50], Contrastive Language-Image Pretraining (CLIP) [51] or other recent models, as the primary goal is to benchmark the performance of VLMs with zero-shot against well-established baselines like VGGNet and ResNet.

## 4.3 Visual Road Assessment and Prompt Design

In this section, we evaluate the framework of our proposed approach, V-RoAst, for examining 52 iRAP attributes from images, as shown in Figure 4. This framework is designed to be easily applicable in any city, requiring minimal data science expertise and coding experience. The approach includes text input for system instructions and prompts, as well as image prompts. The workflow operates by inputting an image and its associated information prompts, including task specifications, local context, attribute details, and output format, to generate responses for the 52 attributes of the image. We used data from ThaiRAP to evaluate the VLMs, as detailed in section 3.

### 4.3.1 Text Prompts

As shown in Figure 5, instructions are divided into 4 parts, including task specification, local context, attribute details, and output format as suggested by OpenAI [52] and Gemini [27] technical report.

1. **Task Specification:** This component provides step-by-step instructions for processing each image. The model is guided to

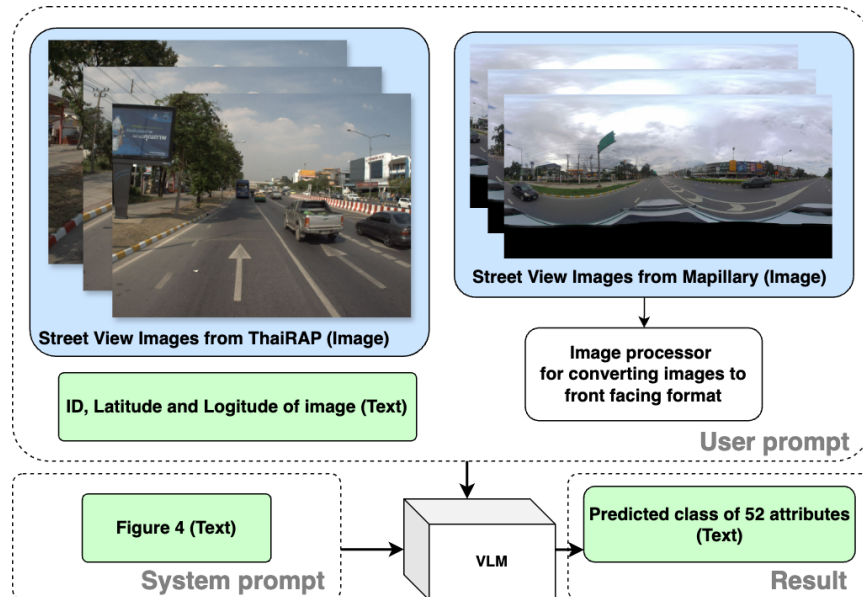


Fig 4. Framework of V-RoAst for Visual Road Assessment

classify each `<Attribute>` by selecting the most appropriate `<Category class>` based on its visual description. This section also specifies how the output should be formatted. Notably, `{country}` is included to localise the analysis for each region.

2. **Local Context:** Contextual details, such as the side of the road on which vehicles drive (left or right), are provided through `{local_context}`. This information helps the VLMs interpret images more accurately. For example, attributes like speed limits or specific infrastructure features are clarified using local regulatory details, enhancing the model's relevance and precision.

Incorporating `{local_context}` is particularly important for attributes that are difficult to classify visually, such as the presence of service roads. This additional input of local context enables the system to account for subtle, location-specific nuances, ensuring robustness in its assessments, as this is to mimic how coders know the area.

3. **Attribute Details:** Each attribute is defined with its name, description (`<Attribute description>`), and possible categories (`<Category class>`), accompanied by descriptions of each category (`<Category description>`). These structured definitions ensure that the models have clear guidelines for classification. Note that this section includes approximately 100,000 characters (or 20,000 tokens) from the iRAP coding manual, which this work made available in JSON format.
4. **Output Format:** The results are returned in JavaScript Object Notation (JSON) format to maintain consistency. The models are instructed to select the best match from the provided `<Category class>` list, making the outputs standardised and interpretable.

<p>You are a road safety assessment coder from the International Road Assessment Programme (IRAP). Your task is to analyse images of road sections taken in <b>{country}</b> and accurately assess 52 road safety attributes. For each attribute, follow these steps:</p> <ol style="list-style-type: none"> <li>1. Analyse the Image: Examine the road section in the image, focusing on all relevant elements that correspond to the 52 '&lt;Attribute&gt;'s you need to assess.</li> <li>2. Read the &lt;Attribute Description&gt;: For each of the 52 attributes, read the '&lt;Attribute description&gt;' to understand what specific aspect of the image you need to evaluate.</li> <li>3. Refer to Categories: For each attribute, refer to the possible '&lt;Category class&gt;' options provided. If a '&lt;Category description&gt;' is available, read it to understand the specific criteria for each category.</li> <li>4. Select the Most Matching Category: Based on your analysis of the image and understanding of the attribute and category descriptions, select the single &lt;Category class&gt; that best matches what you observe in the image. If multiple categories are equally relevant, choose the category that appears first in the provided list.</li> <li>5. Output the Results in JSON Format: Return the results in JSON format, with each attribute associated with a single &lt;Category class&gt; value that you assess to be the most appropriate based on the image.</li> </ol>	<b>Specify Tasks</b>
<p>Local context: '&lt;driver-side&gt;' and '&lt;passenger-side&gt;' are used throughout the &lt;Attribute&gt; and &lt;Attribute description&gt;. Driver-side refers to the side of the road corresponding with the driver of a vehicle travelling in the direction of the survey, and the passenger-side is the other side. If the country drives on the left (e.g., the UK), the passenger side is on the left of the image, and the driver side is on the right of the image.</p> <p><b>{local_context}</b>.</p>	<b>Local Context</b>
<p>1. &lt;Attribute&gt;: Carriageway  &lt;Attribute description&gt;: Record a carriageway label for each section of road to distinguish which carriageway is being coded.  Undivided vs. divided carriageways: Divided (dual) carriageways are surveyed in both directions, but undivided (single) carriageway roads are recorded in one direction only, even if the traffic is two-way. What is considered divided and undivided depends on the median type and its length:  - Divided carriageways are those that physically separate opposing traffic flows by either a barrier or a wide physical median consistently and for a distance of 400m or more.  - An undivided carriageway has no physical separation between opposing traffic flows, or physically separates traffic for a section of less than 400m.  - One-way roads must be coded as undivided and the Median type set to one-way.  - Service roads must be coded separately to the main carriageways. Code service roads the same way as standard roads.  - If a bus or transit lane is part of the main carriageway, code it as part of the carriageway (see instructions on coding transit lanes under Number of lanes). Where there is a dedicated, separated carriageway for buses, these should be coded as divided or undivided carriageways separate to the main carriageway  &lt;Categories&gt;: [Carriageway A of a divided road, Carriageway B of a divided road, Undivided road, Carriageway A of a motorcycle facility, Carriageway B of a motorcycle facility]  &lt;Category class&gt;:Carriageway A of a divided road, &lt;Category description&gt;: Divided carriageway in one direction.  &lt;Category class&gt;:Carriageway B of a divided road, &lt;Category description&gt;: Divided carriageway in opposite direction (to carriageway A).  &lt;Category class&gt;:Undivided road, &lt;Category description&gt;: Undivided carriageway (in both directions or one-way).  &lt;Category class&gt;:Carriageway A of a motorcycle facility, &lt;Category description&gt;: Segregated motorcycle paths adjacent to the main carriageway.  &lt;Category class&gt;:Carriageway B of a motorcycle facility, &lt;Category description&gt;: Segregated motorcycle paths adjacent to the main carriageway.</p> <p>...</p>	<b>Attribute Details</b>
<p>Output format: Return the results in JSON format, where each attribute is associated with a single &lt;Category class&gt; value that best matches your analysis of the image. If multiple categories seem equally relevant, select the category that appears first in the provided list.</p> <p>JSON structure:</p> <pre>{   "image_id": "image_id", "Carriageway": ["Carriageway A of a divided road", "Carriageway B of a divided road", "Undivided road", "Carriageway A of a motorcycle facility", "Carriageway B of a motorcycle facility"],   ... }</pre> <p>Ensure that each attribute in the JSON output contains only one selected &lt;Category class&gt; that you determine to be the most appropriate based on the image.</p>	<b>Output Format</b>

Fig 5. System Prompt from Figure 4

### 4.3.2 Image and Text Prompts

In this experiment, the input combines both image data and accompanying metadata, including `<image_id>:{image_id}` and `<location>:{latitude, longitude}`. These metadata tags help VLMs format the output and enhance contextual understanding.

For example, integrating local speed limit laws allows the VLMs to accurately assess speed-related attributes, such as motorcycle speed limits, truck speed limits, and differential speed limits. This integration ensures that the models consider both visual cues and regulatory context, improving the relevance of the analysis to the local environment and regulation.

By leveraging both visual and textual data, the VLMs can better interpret complex scenes, even in cases where certain attributes are less visually apparent. This dual-input approach enhances the accuracy and reliability of the assessments.

## 4.4 VLMs

This study evaluates Gemini-1.5-flash and GPT-4o-mini for their potential to replicate the work of road safety auditors under the iRAP standard. These models require no additional training or significant computational resources, making them accessible for use by local stakeholders. As demonstrated by [53], Gemini and GPT outperform other models in the Multi-discipline Multimodal Understanding and Reasoning benchmark. The experiments were conducted through the Gemini and the OpenAI API.

To assess their performance, we analysed 337 road segments (1348 images) with Gemini-1.5-flash and GPT-4o-mini, alongside ResNet and VGGNet baseline models. An additional set of 7 segments with unseen attributes was used to evaluate zero-shot classification capabilities.

## 4.5 Image processor for Mapillary imagery

Crowdsourced Street View Images (SVIs) are accessible on various platforms, with Mapillary being one of the most well-known, providing an API for image downloads. Hence, we evaluate the system using the V-RoAst framework with Gemini-1.5-flash to classify all 52 attributes. Then, we combine these results with additional information—including operating speed and ADDT from the ground truth—to determine the star rating outcomes.

For this study, images were obtained using a 50-metre buffer around ThaiRAP locations under the condition that the images were captured within one year of the coding date, as the specific date of the road survey was unavailable. However, only 42 road segments were found to have corresponding Mapillary images, yielding 165 images. Panoramic images were converted to 1200x1600 binocular view images to align with the ThaiRAP data format. Subsequently, these images were processed using V-RoAst to examine attributes, as explained in 4.3.

It is important to note that some attributes may differ from the iRAP ground truth. For example, the number of vehicles shown in the image (observed flow) and the number of vehicles parked in the captured scene can vary. To validate the automatic use of V-RoAst, we did not verify whether the downloaded images originated from the exact same location, which could potentially affect the predicted star rating.

## 4.6 Evaluation Metrics

Our study evaluates performance at two levels: overall model performance and attribute classification performance. Since some coding segments may belong to multiple risk classes, we follow the convention of selecting the first (i.e., highest risk) class listed in the official iRAP coding list.

### 4.6.1 Model Performance Evaluation

To compare the classification outcomes of different models, we calculate the following metrics on a per-attribute basis and aggregate them using a macro-average (i.e., all classes are weighted equally):

**Macro-Accuracy:** The average accuracy computed across all attributes.

**Macro-Precision:** The average precision values computed for each attribute.

**Macro-Recall:** The average recall values computed for each attribute.

**Macro-F1-score:** The average of the F1-scores computed for each attribute, or equivalently, the harmonic mean of macro-Precision and macro-Recall.

#### 4.6.2 Attribute Classification Evaluation

For our VQA task cast as an image classification problem, we evaluate performance on each attribute using the standard metrics defined below:

**Accuracy:** The overall correctness of predictions.

$$\text{Accuracy} = \frac{\text{TP} + \text{TN}}{\text{TP} + \text{TN} + \text{FP} + \text{FN}} \quad (1)$$

**Precision:** The ratio of correctly predicted positive observations to the total predicted positives.

$$\text{Precision} = \frac{\text{TP}}{\text{TP} + \text{FP}} \quad (2)$$

**Recall:** The ratio of correctly predicted positive observations to all observations in the actual class.

$$\text{Recall} = \frac{\text{TP}}{\text{TP} + \text{FN}} \quad (3)$$

**F1-score:** The weighted harmonic mean of Precision and Recall provides a balance between the two.

$$\text{F1-score} = 2 \cdot \frac{\text{Precision} \cdot \text{Recall}}{\text{Precision} + \text{Recall}} \quad (4)$$

Where: TP: True Positives, TN: True Negatives, FP: False Positives, and FN: False Negatives

## 5 Results and Discussions

In this section, we evaluate the attribute classification performance of V-RoAst using Gemini-1.5-flash and GPT-4o-mini, compared to the baselines established by the ResNet and VGGNet models, as used in previous studies [3, 23]. We discuss the overall (macro-averaged) performance as well as insights obtained by examining performance on individual attributes.

## 5.1 Overall (Macro) Performance

The following table (Table 1) summarises the macro-averaged performance metrics (Accuracy, Precision, Recall, and F1-score) for each model. The ResNet model shows the highest overall performance with a macro-accuracy of 96.23% and macro-precision, recall, and F1-scores of 88.39%, 85.66%, and 86.32%, respectively. VGGNet is very close in terms of accuracy at 95.61%, but its macro-precision, recall, and F1-scores (76.44%, 74.44%, and 74.83%) are relatively lower. This indicates that while both models achieve high overall accuracy, ResNet is more reliable in correctly identifying positive cases and reducing false positives.

The VLMs with zero-shot show a drop in performance compared to the baseline models. Gemini-1.5-flash has a macro-accuracy of 81.82% and macro-precision and recall around 49%, with a macro-F1-score of 47.15%. GPT-4o-mini performs slightly worse.

While baseline models provide higher macro-averaged performance metrics, they are limited to a fixed set of classes determined during training. In contrast, VLMs, although scoring lower in these metrics, offer the advantage of predicting from all possible classes rather than being confined to the classes seen during training.

**Table 1.** Macro-averaged Performance Metrics for Each Model. All metrics are expressed as percentages.

Model	Accuracy	Precision	Recall	F1-score
ResNet	96.23%	88.39%	85.66%	86.32%
VGGNet	95.61%	76.44%	74.44%	74.83%
Gemini-1.5-flash	<b>81.82%</b>	<b>49.32%</b>	<b>49.68%</b>	<b>47.15%</b>
GPT-4o-mini	75.11%	46.48%	46.75%	41.81%

## 5.2 Attribute-Level Performance

Figure 6 presents the performance metrics, including Accuracy, Precision, Recall, and F1-score for all four models, with a colour scale indicating performance bands. Note that the baseline models (VGGNet and ResNet) excluded 11 attributes because their training datasets contained only a single class for those attributes. V-RoAst, on the other hand, overcomes this limitation by not requiring a training dataset for each attribute, allowing it to select from all possible classes.

The baseline models demonstrate higher performance for spatially dependent attributes, such as road severity distance and object, particularly in tasks like distance estimation and determining the relationship between the closest and riskiest object among 50. Their specialised training enables them to capture subtle spatial nuances more effectively. In contrast, VLMs rely on logical reasoning, a capability that may improve with in-context learning.

On the other hand, VLMs show relatively good performance on non-spatial attributes, effectively identifying the presence or absence of prominent objects or features, even when evaluated on previously unseen datasets. However, both approaches exhibit limitations when it comes to ambiguous or complex attributes, with the gap between the VLMs and the baseline models becoming more pronounced in these scenarios.

Attribute	Accuracy				Precision				Recall				F1-Score				
	ResNet	VGG	Gemini	GPT	ResNet	VGG	Gemini	GPT	ResNet	VGG	Gemini	GPT	ResNet	VGG	Gemini	GPT	
Area type	98.36	95.90	81.90	90.21	100.00	100.00	65.68	67.56	100.00	100.00	85.68	85.68	58.37	100.00	100.00	68.46	60.71
Bicycle (OF)			100.00	100.00			100.00	100.00			100.00	100.00			100.00	100.00	
Carriageway	100.00	100.00	98.52	98.52	100.00	100.00	49.85	49.85	100.00	100.00	49.40	49.40	100.00	100.00	49.63	49.63	
Centreline rumble strips	100.00	100.00					100.00	100.00			100.00	100.00			100.00	100.00	
Curvature	98.77	98.98	98.22	97.92	100.00	50.00	62.05	49.40	100.00	48.00	62.05	49.55	100.00	49.00	62.05	49.48	
Delineation	100.00	99.80	99.70	99.70	100.00	50.00	49.85	49.85	100.00	48.00	50.00	50.00	100.00	49.00	49.93	49.93	
Differential speed limits	98.36	98.98	74.48	21.36	97.00	100.00	39.47	60.09	96.00	100.00	46.48	50.93	97.00	100.00	42.69	18.61	
(F) for bicycles			100.00	100.00			100.00	100.00			100.00	100.00			100.00	100.00	
(F) for motorised two wheelers			100.00	99.70			100.00	50.00			100.00	49.85			100.00	49.93	
Grade			100.00	100.00			100.00	100.00			100.00	100.00			100.00	100.00	
Intersecting road volume	94.26	94.26	93.18	93.18	98.00	100.00	23.57	15.72	75.00	100.00	24.69	16.46	83.00	100.00	24.12	16.08	
Intersection channelisation	100.00	100.00	99.41	98.81	100.00	100.00	49.85	49.85	100.00	100.00	49.85	49.55	100.00	100.00	49.85	49.70	
Intersection quality	94.06	94.06	93.18	93.18	100.00	100.00	31.43	47.15	100.00	100.00	32.91	49.37	100.00	100.00	32.16	48.23	
Intersection type	94.06	94.26	92.58	92.58	100.00	100.00	15.62	18.74	100.00	100.00	16.46	19.75	100.00	100.00	16.02	19.23	
Land use - (DS)	100.00	100.00	98.52	37.98	100.00	100.00	33.23	33.49	100.00	100.00	32.94	45.93	100.00	100.00	33.08	18.60	
Land use - (PS)	87.70	85.66	26.41	70.03	55.00	55.00	20.52	25.59	54.00	53.00	17.27	31.28	54.00	54.00	10.72	26.68	
Lane width			100.00	100.00			100.00	100.00			100.00	100.00			100.00	100.00	
Median type	94.67	93.24	72.40	18.99	97.00	67.00	21.42	16.52	84.00	70.00	25.05	22.12	89.00	68.00	22.86	8.00	
Motorcycle (OF)	96.31	95.70	92.88	79.53	67.00	48.00	57.69	20.31	97.00	48.00	42.39	26.88	73.00	48.00	46.08	20.04	
Motorcycle speed limit	99.59	99.80	96.14	54.30	100.00	48.00	85.96	55.49	100.00	50.00	73.21	75.79	100.00	49.00	78.02	43.92	
Number of lanes	94.88	94.88	55.49	13.65	82.00	66.00	29.76	29.00	82.00	44.00	54.20	31.85	82.00	49.00	25.87	9.05	
Paved shoulder - (DS)	96.11	97.54	1.78	11.28	88.00	91.00	25.00	22.09	84.00	91.00	0.52	3.31	86.00	91.00	1.02	5.76	
Paved shoulder - (PS)	88.93	86.89	40.65	18.99	98.00	86.00	31.08	9.20	94.00	87.00	26.52	11.35	96.00	86.00	24.97	10.16	
(PC) (F) - inspected road	96.11	94.47	94.66	94.07	48.00	48.00	56.63	31.36	47.00	48.00	38.78	33.33	48.00	48.00	41.50	32.31	
(PC) (F) - intersecting road	99.18	99.39	98.81	98.81	100.00	100.00	32.94	32.94	100.00	100.00	33.33	33.33	100.00	100.00	33.13	33.13	
(PC) quality	95.29	94.67	93.47	93.47	48.00	48.00	46.74	46.74	47.00	48.00	50.00	50.00	48.00	48.00	48.31	48.31	
Pedestrian fencing	100.00	100.00	99.70	99.70	100.00	100.00	49.85	49.85	100.00	100.00	50.00	50.00	100.00	100.00	49.93	49.93	
(POF) across the road			100.00	99.70			100.00	50.00			100.00	49.85			100.00	49.93	
(POF) along the road (DS)	100.00	100.00	98.81	99.11	100.00	100.00	33.13	33.13	100.00	100.00	33.13	33.23	100.00	100.00	33.13	33.18	
(POF) along the road (PS)	100.00	100.00	99.41	99.11	100.00	100.00	49.70	33.13	100.00	100.00	50.00	33.23	100.00	100.00	49.85	33.18	
Property access points	94.06	93.65	87.54	82.49	98.00	97.00	38.73	37.05	83.00	67.00	26.08	36.45	89.00	73.00	25.69	36.63	
Quality of curve	98.77	98.98	98.22	97.92	100.00	50.00	62.05	49.40	100.00	48.00	62.05	49.55	100.00	49.00	62.05	49.48	
Road condition			97.92	99.11			50.00	50.00			48.96	49.55			49.48	49.78	
(RS) - (DS) distance	95.90	96.52	0.00	13.35	94.00	91.00	0.00	24.91	98.00	91.00	0.00	16.51	96.00	91.00	0.00	10.03	
(RS) - (DS) object	94.47	92.62	81.60	24.63	46.00	46.00	27.30	17.83	48.00	48.00	29.12	9.79	47.00	47.00	28.15	9.70	
(RS) - (PS) distance	87.70	85.66	3.86	36.20	66.00	60.00	2.72	39.19	52.00	58.00	26.34	37.81	55.00	57.00	4.43	22.47	
(RS) - (PS) object	76.02	70.70	26.11	23.74	89.00	82.00	6.07	29.06	87.00	80.00	16.08	26.14	88.00	80.00	8.51	16.30	
Roadworks			99.11	99.70			50.00	50.00			49.55	49.85			49.78	49.93	
(SZ) crossing supervisor	98.16	96.11	95.85	96.14	98.00	73.00	32.04	48.07	75.00	73.00	33.23	50.00	83.00	73.00	32.63	49.02	
(SZ) warning	98.16	96.31	95.85	96.14	98.00	98.00	32.04	48.07	75.00	75.00	33.23	50.00	83.00	83.00	32.63	49.02	
Service road	97.95	96.72	9.79	11.87	98.00	47.00	4.90	55.00	75.00	50.00	50.00	51.15	83.00	48.00	8.92	11.34	
Shoulder rumble strips	98.36	98.98	95.85	99.41	48.00	48.00	49.69	49.70	50.00	50.00	48.21	50.00	49.00	49.00	48.94	49.85	
Sidewalk - (DS)			97.92	89.32			33.33	50.00			32.64	44.66			32.98	47.18	
Sidewalk - (PS)	93.03	91.60	83.38	77.45	72.00	34.00	30.71	18.20	74.00	32.00	19.61	21.30	73.00	33.00	20.24	19.56	
Sight distance			100.00	100.00			100.00	100.00			100.00	100.00			100.00	100.00	
Skid resistance / grip	99.18	98.16	80.12	79.82	98.00	98.00	73.45	39.91	95.00	95.00	51.28	50.00	96.00	96.00	47.26	44.39	
Speed limit	98.36	98.98	74.18	43.92	98.00	65.00	50.26	33.63	97.00	67.00	47.79	33.41	98.00	66.00	47.59	29.51	
Speed management	96.31	97.95	80.42	80.42	97.00	100.00	40.21	40.21	96.00	100.00	50.00	50.00	97.00	100.00	44.57	44.57	
Street lighting	97.13	96.11	94.07	89.32	100.00	100.00	74.59	61.66	100.00	100.00	72.39	67.63	100.00	100.00	73.42	63.76	
Truck speed limit	99.80	99.80	94.07	62.31	100.00	48.00	57.29	38.29	100.00	50.00	48.07	51.70	100.00	49.00	51.64	33.87	
Upgrade cost	95.90	93.44	61.42	49.26	98.00	92.00	38.76	56.67	97.00	83.00	44.99	34.36	97.00	86.00	40.38	24.53	
Vehicle parking	99.59	99.39	97.33	79.23	48.00	48.00	49.70	33.21	50.00	50.00	48.96	26.57	49.00	49.00	49.32	29.52	
Zero-Shot Prediction on Unseen Dataset																	
Intersection channelisation	14.29	14.29	85.71	85.71	5.00	5.00	91.67	91.67	33.00	33.00	75.00	75.00	8.00	8.00	78.79	78.79	
Intersection type	3.57	0.00	71.43	71.43	50.00	0.00	20.83	20.83	2.00	0.00	25.00	25.00	3.00	0.00	22.73	22.73	
(PC) quality	7.14	0.00	57.14	57.14	50.00	0.00	28.57	28.57	4.00	0.00	50.00	50.00	7.00	0.00	36.36	36.36	
Property access points	3.57	0.00	85.71	71.43	11.00	0.00	91.67	65.00	2.00	0.00	75.00	65.00	3.00	0.00	78.79	65.00	
(RS) - (DS) distance	85.71	82.14	0.00	0.00	92.00	81.00	0.00	0.00	75.00	72.00	0.00	0.00	79.00	75.00	0.00	0.00	
(RS) - (DS) object	57.14	46.43	71.43	0.00	26.00	24.00	35.42	0.00	33.00	33.00	50.00	0.00	28.00	27.00	41.43	0.00	

**Fig 6.** Accuracy, Precision, Recall, and F1-score of ResNet, VGGNet, Gemini-1.5-flash, and GPT-4o-mini. All performance metrics are expressed as percentages (0–100). The colour scale represents performance as follows: 80–100% (Green), 60–79% (Light Green), 40–59% (Yellow), 20–39% (Orange), and below 20% (Red).

In summary, while baseline models show strong macro-averaged results, V-RoAst’s ability to handle all attributes makes it a promising tool for road safety assessment. Future work might explore hybrid models that leverage the strengths of both VLMs and supervised approaches to address the unique challenges presented by different attribute types. This trade-off suggests that integrating the strengths of both approaches—using supervised models for spatially and quantitatively precise tasks and VLMs for handling diverse, potentially unseen attribute classes—could lead to

improved overall performance in road safety assessment. Importantly, VLMs might help preclassify attributes when the results are appropriate, which can then be used to train supervised models later.

### 5.3 Qualitative Assessment using VQA

One major advantage of using LVLMs is their ability to perform Visual Question Answering (VQA), allowing users with minimal technical expertise to enhance model predictions through prompt refinement. This iterative process enables stakeholders to adapt prompts intuitively based on how LVLMs interpret text and image inputs, as illustrated in Figure 7.

For instance, in the bottom right of Figure 7, models such as VGGNet, ResNet, Gemini-1.5-flash, and GPT-4o-mini failed to classify the attribute "Sidewalk-passenger-side accurately." The ground truth indicated an informal path more than 1 metre from the road, which was not visually apparent in the image. The lack of sufficient visual cues necessitated input from local coders familiar with the assessed roads. To address such gaps, incorporating additional data sources, such as satellite imagery, could provide valuable context and improve model performance.



**Fig 7.** Qualitative assessment of VLM performance using VQA with correct (green) and wrong (red) answers

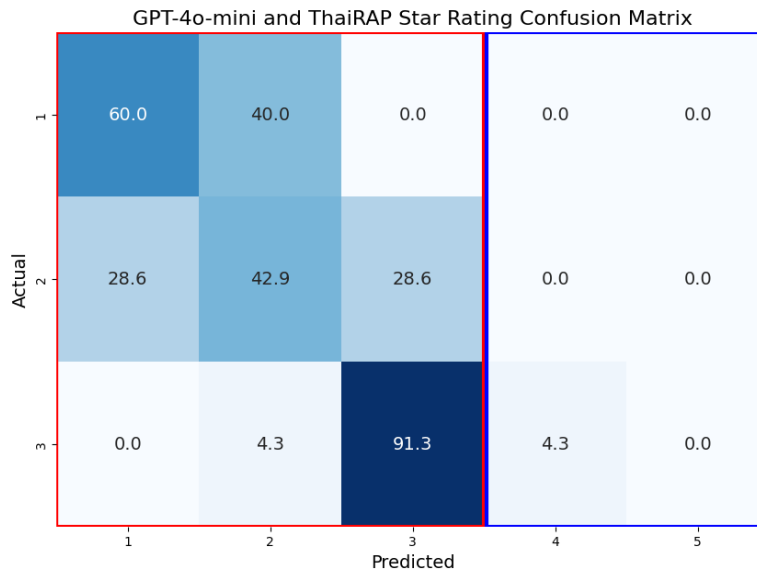
### 5.4 Scalable Star Rating Prediction

Figure 8 presents the confusion matrix for star rating predictions (motorcyclists) using Mapillary images with V-RoAst and Gemini-1.5-flash.

The results demonstrate the model’s effectiveness in identifying high-risk roads with star ratings below 3, highlighted in the red box.

The flexibility of the V-RoAst framework lies in its integration of `{local_context}`, allowing local stakeholders to tailor prompts based on their expertise and validate results against ground truth data. This adaptability enables precise identification of high-risk areas, supporting road safety initiatives and investment prioritisation. Although Mapillary’s current coverage is limited, its crowdsourced platform serves as a valuable resource that transport authorities can leverage [54, 55]. Similar applications using commercial platforms like Google Street View may be explored, subject to licensing agreements.

To achieve comprehensive safety assessments, additional inputs such as Annual Average Daily Traffic (AADT) and operating speeds, as outlined in the iRAP Star Rating and Investment Plan Manual<sup>6</sup>, are essential. While these variables are not derived directly from SVI labels, they play a critical role in determining road safety performance and star ratings.



**Fig 8.** Star rating (motorcyclists) confusion matrix of using crowdsourced imagery with V-RoAst and ground truth from ThaiRAP

## 6 Conclusion and Future work

In this study, we proposed the V-RoAst, which utilises zero-shot prompting with Visual Language Models (VLMs) including Gemini-1.5-flash and GPT-4o-mini. We compared their performance with traditional CNN models like ResNet and VGGNet. The results indicate that while our approach shows promise in classifying road attributes, it currently underperforms compared to traditional CNN models. However, VLMs offer the additional benefit of performing Visual Question Answering (VQA), which provides opportunities for intuitive prompt engineering and future improvements in accuracy and robustness. This capability is particularly

<sup>6</sup>[https://resources.irap.org/Specifications/iRAP\\_Star\\_Rating\\_and\\_Investment\\_Plan\\_Manual\\_English.pdf](https://resources.irap.org/Specifications/iRAP_Star_Rating_and_Investment_Plan_Manual_English.pdf)

beneficial for local authorities in LMICs, where resource constraints make the adaptability and ease of use of VLMs highly advantageous.

While VLMs show potential in automating road safety assessments, particularly for easily interpretable attributes, challenges remain in fully aligning them with the iRAP standard. For instance, VLMs demonstrate relatively weaker performance when dealing with spatially complex attributes, where local context or additional data sources (e.g., satellite imagery or geographical data) may be required to improve accuracy. Furthermore, the inability of VLMs to consistently classify attributes requiring implicit knowledge, such as "Sidewalk-passenger-side" in cases of informal paths, highlights the need for further development. As demonstrated in Figure 7, ensuring comprehensive coverage of street features in street view images is essential. For example, suppose the sidewalk on the passenger side is not visible in the image. In that case, it becomes impossible for either VLMs or traditional CNN models to accurately classify their presence, regardless of their training or capabilities. In such cases, integrating satellite images as a complementary data source may help provide additional context and fill gaps in the visual information, thereby supporting more robust model performance.

The findings suggest that VLMs could play a significant role as road safety assessors under the iRAP standard, particularly when complementing existing methods. However, to fully realise their potential, future work should focus on the following areas:

- **In-context Learning:** Applying few-shot [56] or Chain of Thought [57] prompting to improve the classification.
- **Supervised Fine-tuning VLMs:** Adapting image-text pre-training models using (LoRA) [58], for example, LLaMa3 [59] to handle a broader range of road safety attributes, particularly those requiring nuanced spatial understanding or integration of local knowledge.
- **Incorporating additional modalities:** Enhancing VLM capabilities by integrating remote sensing imagery, GIS data, and other complementary datasets to address gaps in visual cues, as demonstrated by the potential of RemoteCLIP [60].
- **Cross-regional generalisability:** Ensuring robustness and versatility of VLMs across diverse geographical and socio-economic contexts, regardless of the country, to make them globally applicable.
- **User-friendly interfaces for local authorities:** Developing tools that allow non-expert stakeholders to interact with VLMs intuitively, such as through enhanced prompt engineering or automated workflows.

In conclusion, while VLMs may not yet fully replace trained road safety coders in adhering to the iRAP standard, their integration into road safety assessments shows great potential. By addressing current limitations and leveraging their strengths, VLMs could evolve into powerful tools for improving road safety globally, especially in regions where resources and expertise are limited.

## Acknowledgments

We would like to thank the Thai Road Assessment Programme (ThaiRAP) for providing the dataset.

## References

1. WHO. Global status report on road safety 2023. Geneva: World Health Organization; 2023. Available from: <https://iris.who.int/>.
2. Chen S, Kuhn M, Prettner K, Bloom DE. The global macroeconomic burden of road injuries: estimates and projections for 166 countries. *The Lancet Planetary Health*. 2019;3(9):e390–e398. doi:10.1016/S2542-5196(19)30170-6.
3. Kacan M, Orsic M, Segvic S, Sevrovic M. Multi-Task Learning for iRAP Attribute Classification and Road Safety Assessment. In: 2020 IEEE 23rd International Conference on Intelligent Transportation Systems (ITSC). Rhodes, Greece: IEEE; 2020. p. 1–6. Available from: <https://ieeexplore.ieee.org/document/9294305/>.
4. Pubudu Sanjeevani TG, Verma B. Learning and Analysis of AusRAP Attributes from Digital Video Recording for Road Safety. In: 2019 International Conference on Image and Vision Computing New Zealand (IVCNZ). Dunedin, New Zealand: IEEE; 2019. p. 1–6. Available from: <https://ieeexplore.ieee.org/document/8960997/>.
5. Jan Z, Verma B, Affum J, Atabak S, Moir L. A Convolutional Neural Network Based Deep Learning Technique for Identifying Road Attributes. In: 2018 International Conference on Image and Vision Computing New Zealand (IVCNZ). Auckland, New Zealand: IEEE; 2018. p. 1–6. Available from: <https://ieeexplore.ieee.org/document/8634743/>.
6. Sanjeevani P, Verma B. Single class detection-based deep learning approach for identification of road safety attributes. *Neural Computing and Applications*. 2021;33(15):9691–9702. doi:10.1007/s00521-021-05734-z.
7. Sanjeevani P, Verma B. Optimization of Fully Convolutional Network for Road Safety Attribute Detection. *IEEE Access*. 2021;9:120525–120536. doi:10.1109/ACCESS.2021.3108543.
8. Brkić I, Miler M, Ševrović M, Medak D. Automatic Roadside Feature Detection Based on Lidar Road Cross Section Images. *Sensors*. 2022;22(15):5510. doi:10.3390/s22155510.
9. Brkić I, Ševrović M, Medak D, Miler M. Utilizing High Resolution Satellite Imagery for Automated Road Infrastructure Safety Assessments. *Sensors*. 2023;23(9):4405. doi:10.3390/s23094405.
10. Abdollahi A, Pradhan B, Shukla N, Chakraborty S, Alamri A. Deep Learning Approaches Applied to Remote Sensing Datasets for Road Extraction: A State-Of-The-Art Review. *Remote Sensing*. 2020;12(9):1444. doi:10.3390/rs12091444.
11. Brkić I, Miler M, Ševrović M, Medak D. An Analytical Framework for Accurate Traffic Flow Parameter Calculation from UAV Aerial Videos. *Remote Sensing*. 2020;12(22):3844. doi:10.3390/rs12223844.

12. Yin Y, Hu W, Tran A, Zhang Y, Wang G, Kruppa H, et al. Multimodal Deep Learning for Robust Road Attribute Detection. *ACM Transactions on Spatial Algorithms and Systems*. 2023;9(4):1–25. doi:10.1145/3618108.
13. Lewis P, Perez E, Piktus A, Petroni F, Karpukhin V, Goyal N, et al.. Retrieval-Augmented Generation for Knowledge-Intensive NLP Tasks; 2021. Available from: <http://arxiv.org/abs/2005.11401>.
14. Xing J, Liu J, Wang J, Sun L, Chen X, Gu X, et al. A survey of efficient fine-tuning methods for Vision-Language Models — Prompt and Adapter. *Computers & Graphics*. 2024;119:103885. doi:10.1016/j.cag.2024.01.012.
15. Zeng Z, Goo JM, Wang X, Chi B, Wang M, Boehm J. Zero-Shot Building Age Classification from Facade Image Using GPT-4. *The International Archives of the Photogrammetry, Remote Sensing and Spatial Information Sciences*. 2024;XLVIII-2-2024:457–464. doi:10.5194/isprs-archives-XLVIII-2-2024-457-2024.
16. Goo JM, Zeng Z, Boehm J. Zero-Shot Detection of Buildings in Mobile LiDAR using Language Vision Model. *The International Archives of the Photogrammetry, Remote Sensing and Spatial Information Sciences*. 2024;XLVIII-2-2024:107–113. doi:10.5194/isprs-archives-XLVIII-2-2024-107-2024.
17. Jongwiriyannurak N, Zeng Z, Wang M, Haworth J, Tanaksaranond G, Boehm J. Framework for Motorcycle Risk Assessment Using Onboard Panoramic Camera. In: *12th International Conference on Geographic Information Science (GIScience 2023)*; 2023.
18. Wu M, Huang Q, Gao S, Zhang Z. Mixed land use measurement and mapping with street view images and spatial context-aware prompts via zero-shot multimodal learning. *International Journal of Applied Earth Observation and Geoinformation*. 2023;125:103591. doi:10.1016/j.jag.2023.103591.
19. Yong G, Jeon K, Gil D, Lee G. Prompt engineering for zero-shot and few-shot defect detection and classification using a visual-language pretrained model. *Computer-Aided Civil and Infrastructure Engineering*. 2023;38(11):1536–1554. doi:10.1111/mice.12954.
20. Goo JM, Milidonis X, Artusi A, Boehm J, Ciliberto C. Hybrid-Segmentor: Hybrid approach for automated fine-grained crack segmentation in civil infrastructure. *Automation in Construction*. 2025;170:105960. doi:10.1016/j.autcon.2024.105960.
21. Ma N, Fan J, Wang W, Wu J, Jiang Y, Xie L, et al. Computer vision for road imaging and pothole detection: a state-of-the-art review of systems and algorithms. *Transportation Safety and Environment*. 2022;4(4):tdac026. doi:10.1093/tse/tdac026.
22. Ibragimov E, Lee HJ, Lee JJ, Kim N. Automated pavement distress detection using region based convolutional neural networks. *International Journal of Pavement Engineering*. 2022;23(6):1981–1992. doi:10.1080/10298436.2020.1833204.

23. Song W, Workman S, Hadzic A, Zhang X, Green E, Chen M, et al. FARSA: Fully Automated Roadway Safety Assessment. In: 2018 IEEE Winter Conference on Applications of Computer Vision (WACV). Lake Tahoe, NV: IEEE; 2018. p. 521–529. Available from: <https://ieeexplore.ieee.org/document/8354167/>.
24. Kačan M, Ševrović M, Šegvić S. Dynamic Loss Balancing and Sequential Enhancement for Road-Safety Assessment and Traffic Scene Classification. *IEEE Transactions on Intelligent Transportation Systems*. 2024;25(11):15628–15640. doi:10.1109/TITS.2024.3456214.
25. Hendrycks D, Gimpel K. A Baseline for Detecting Misclassified and Out-of-Distribution Examples in Neural Networks; 2018. Available from: <http://arxiv.org/abs/1610.02136>.
26. OpenAI. GPT-4o System Card; 2024. Available from: <https://cdn.openai.com/gpt-4o-system-card.pdf>.
27. Gemini T. Gemini 1.5: Unlocking multimodal understanding across millions of tokens of context; 2024. Available from: <http://arxiv.org/abs/2403.05530>.
28. Wang W, Lv Q, Yu W, Hong W, Qi J, Wang Y, et al.. CogVLM: Visual Expert for Pretrained Language Models; 2024. Available from: <http://arxiv.org/abs/2311.03079>.
29. Liu H, Li C, Wu Q, Lee YJ. Visual Instruction Tuning; 2023. Available from: <http://arxiv.org/abs/2304.08485>.
30. Touvron H, Lavril T, Izacard G, Martinet X, Lachaux MA, Lacroix T, et al.. LLaMA: Open and Efficient Foundation Language Models; 2023. Available from: <http://arxiv.org/abs/2302.13971>.
31. Bai J, Bai S, Yang S, Wang S, Tan S, Wang P, et al.. Qwen-VL: A Versatile Vision-Language Model for Understanding, Localization, Text Reading, and Beyond; 2023. Available from: <http://arxiv.org/abs/2308.12966>.
32. Siddiqui Y, Alliegro A, Artemov A, Tommasi T, Sirigatti D, Rosov V, et al.. MeshGPT: Generating Triangle Meshes with Decoder-Only Transformers; 2023. Available from: <http://arxiv.org/abs/2311.15475>.
33. Hoyer L, Tan DJ, Naeem MF, Van Gool L, Tombari F. SemiVL: Semi-Supervised Semantic Segmentation with Vision-Language Guidance; 2023. Available from: <http://arxiv.org/abs/2311.16241>.
34. Min C, Zhao D, Xiao L, Zhao J, Xu X, Zhu Z, et al.. DriveWorld: 4D Pre-trained Scene Understanding via World Models for Autonomous Driving; 2024. Available from: <http://arxiv.org/abs/2405.04390>.
35. Wang Y, He J, Fan L, Li H, Chen Y, Zhang Z. Driving into the Future: Multiview Visual Forecasting and Planning with World Model for Autonomous Driving; 2023. Available from: <http://arxiv.org/abs/2311.17918>.

36. Yang H, Zhang S, Huang D, Wu X, Zhu H, He T, et al.. UniPAD: A Universal Pre-training Paradigm for Autonomous Driving; 2024. Available from: <http://arxiv.org/abs/2310.08370>.
37. Wang S, Yu Z, Jiang X, Lan S, Shi M, Chang N, et al.. OmniDrive: A Holistic LLM-Agent Framework for Autonomous Driving with 3D Perception, Reasoning and Planning; 2024. Available from: <http://arxiv.org/abs/2405.01533>.
38. Xu Z, Zhang Y, Xie E, Zhao Z, Guo Y, Wong KYK, et al. DriveGPT4: Interpretable End-to-End Autonomous Driving Via Large Language Model. *IEEE Robotics and Automation Letters*. 2024;9(10):8186–8193. doi:10.1109/LRA.2024.3440097.
39. Wen L, Yang X, Fu D, Wang X, Cai P, Li X, et al.. On the Road with GPT-4V(ision): Early Explorations of Visual-Language Model on Autonomous Driving; 2023. Available from: <http://arxiv.org/abs/2311.05332>.
40. Luo S, Chen W, Tian W, Liu R, Hou L, Zhang X, et al. Delving Into Multi-Modal Multi-Task Foundation Models for Road Scene Understanding: From Learning Paradigm Perspectives. *IEEE Transactions on Intelligent Vehicles*. 2024; p. 1–25. doi:10.1109/TIV.2024.3406372.
41. Agrawal A, Lu J, Antol S, Mitchell M, Zitnick CL, Batra D, et al.. VQA: Visual Question Answering; 2016. Available from: <http://arxiv.org/abs/1505.00468>.
42. Hudson DA, Manning CD. GQA: A New Dataset for Real-World Visual Reasoning and Compositional Question Answering; 2019. Available from: <http://arxiv.org/abs/1902.09506>.
43. Marino K, Rastegari M, Farhadi A, Mottaghi R. OK-VQA: A Visual Question Answering Benchmark Requiring External Knowledge; 2019. Available from: <http://arxiv.org/abs/1906.00067>.
44. Hendrycks D, Burns C, Basart S, Zou A, Mazeika M, Song D, et al.. Measuring Massive Multitask Language Understanding; 2021. Available from: <http://arxiv.org/abs/2009.03300>.
45. Geiger A, Lenz P, Stiller C, Urtasun R. Vision meets robotics: The KITTI dataset. *The International Journal of Robotics Research*. 2013;32(11):1231–1237. doi:10.1177/0278364913491297.
46. Qian T, Chen J, Zhuo L, Jiao Y, Jiang YG. NuScenes-QA: A Multi-Modal Visual Question Answering Benchmark for Autonomous Driving Scenario. *Proceedings of the AAAI Conference on Artificial Intelligence*. 2024;38(5):4542–4550. doi:10.1609/aaai.v38i5.28253.
47. Jain S, Thapa S, Chen KT, Abbott AL, Sarkar A. Semantic Understanding of Traffic Scenes with Large Vision Language Models. In: 2024 IEEE Intelligent Vehicles Symposium (IV). Jeju Island, Korea, Republic of: IEEE; 2024. p. 1580–1587. Available from: <https://ieeexplore.ieee.org/document/10588373/>.

48. Simonyan K, Zisserman A. Very Deep Convolutional Networks for Large-Scale Image Recognition; 2015. Available from: <http://arxiv.org/abs/1409.1556>.
49. He K, Zhang X, Ren S, Sun J. Deep Residual Learning for Image Recognition; 2015. Available from: <http://arxiv.org/abs/1512.03385>.
50. Radford A, Kim JW, Hallacy C, Ramesh A, Goh G, Agarwal S, et al.. Learning Transferable Visual Models From Natural Language Supervision; 2021. Available from: <http://arxiv.org/abs/2103.00020>.
51. Dosovitskiy A, Beyer L, Kolesnikov A, Weissenborn D, Zhai X, Unterthiner T, et al.. An Image is Worth 16x16 Words: Transformers for Image Recognition at Scale; 2021. Available from: <http://arxiv.org/abs/2010.11929>.
52. OpenAI. GPT-4 Technical Report; 2024. Available from: <http://arxiv.org/abs/2303.08774>.
53. Yue X, Ni Y, Zhang K, Zheng T, Liu R, Zhang G, et al.. MMMU: A Massive Multi-discipline Multimodal Understanding and Reasoning Benchmark for Expert AGI; 2024. Available from: <http://arxiv.org/abs/2311.16502>.
54. Wang M, Haworth J, Chen H, Liu Y, Shi Z. Investigating the potential of crowdsourced street-level imagery in understanding the spatiotemporal dynamics of cities: A case study of walkability in Inner London. *Cities*. 2024;153:105243. doi:10.1016/j.cities.2024.105243.
55. Hou Y, Quintana M, Khomiakov M, Yap W, Ouyang J, Ito K, et al. Global Streetscapes — A comprehensive dataset of 10 million street-level images across 688 cities for urban science and analytics. *ISPRS Journal of Photogrammetry and Remote Sensing*. 2024;215:216–238.
56. Brown TB, Mann B, Ryder N, Subbiah M, Kaplan J, Dhariwal P, et al. Language Models are Few-Shot Learners. In: 34th Conference on Neural Information Processing Systems (NeurIPS 2020); 2022.
57. Wei J, Wang X, Schuurmans D, Bosma M, Ichter B, Xia F, et al.. Chain-of-Thought Prompting Elicits Reasoning in Large Language Models; 2023. Available from: <http://arxiv.org/abs/2201.11903>.
58. Hu EJ, Shen Y, Wallis P, Allen-Zhu Z, Li Y, Wang S, et al.. LoRA: Low-Rank Adaptation of Large Language Models; 2021. Available from: <http://arxiv.org/abs/2106.09685>.
59. Llama T. The Llama 3 Herd of Models; 2024. Available from: <http://arxiv.org/abs/2407.21783>.
60. Liu F, Chen D, Guan Z, Zhou X, Zhu J, Ye Q, et al. RemoteCLIP: A Vision Language Foundation Model for Remote Sensing. *IEEE Transactions on Geoscience and Remote Sensing*. 2024;62:1–16. doi:10.1109/TGRS.2024.3390838.